# Assessing the economic impacts of a 'perfect storm' of extreme weather, pandemic control and deglobalization: a methodological construct

Yixin Hu, Daoping Wang, Jingwen Huo, Lili Yang, Dabo Guan, Paul Brenton and Vicky Chemutai

Abstract

This paper investigates the economic impacts of a multi-disaster mix comprising of extreme weather, such as flooding, a pandemic and deglobalization, dubbed a "perfect storm". We develop a compound-hazard impact model that improves on the standard ARIO model, which is commonly used in single-hazard impact analysis, by considering the interplay between different types of hazardous events. The model also allows for substitution between suppliers of the same sector from different regions, which can influence the resilience of the economic network to multiple shocks. We explore a range of scenarios to investigate economic impacts when flooding and a pandemic collide and how these are affected by the spatial spread, the duration and the strictness of the measures to control the pandemic. In addition, we look at how export restrictions, reflecting deglobalization and measures that were introduced during the COVID pandemic impact of the economic losses and recovery, especially when there is specialization of production of key sectors. The results show that regional or global cooperation is needed to address the spillover effects of such compound events, especially in the context of the risks from deglobalization.

## 1. Introduction

During the past year the escalating COVID-19 pandemic appeared to have diverted attention away from the climate crisis (Selby & Kagawa, 2020; The Lancet, 2020), despite the fact that just a few years prior, the WHO had identified climate change as 'the greatest threat to global health in the 21st century' (World Health Organization (WHO), 2015). Actually, the year 2020 saw a number of climate disasters. It has been reported to have been the hottest year on record (Gohd, 2021). The dry and hot conditions fueled massive record-breaking wildfires across Australia, Siberia, and the United States. The 2020 Atlantic hurricane season was also the most active in recorded history (White, 2020). Devastating typhoons swamped the Indian subcontinent and south-east Asia while the Sahel and Greater Horn regions of Africa experienced severe droughts (Boyle, 2020). and devastation from locust swarms linked to climate change.[1] Early 2021 also saw the Swiss Alps develop an orange layer caused by heavy sandstorms from the Sahara Desert, the widest reach recorded in recent years.[2]

Several aspects signaling deglobalization have been at play in recent years. The 2020 World Development Report reports that growth in global value chains has flattened. Additionally, country and regional reform agendas have either experienced a reversal or have stalled. China's recent move towards promoting local industries and the falling share of exports as a share of GDP (from 31 percent in 2008 to just 17 percent in 2019) further brightens this signal. 2020 also saw increasing trade tensions, especially in relations between the US and China, as well as the UK withdrawing from the EU, but also in some of the responses by governments to the pandemic. Indeed, some have argued that the pandemic has further fueled the process of deglobalization. On the other hand, trade in goods has recovered well as consumers shift purchases away from services such as hospitality and travel and global value chains in many sectors, with notable exceptions such as apparel, appear to have be somewhat resilient.[3] Nevertheless, a number of countries have responded by introducing export restrictions on critical medical equipment and food and even on vaccines. This raises the issue of whether restrictive trade policy measures can undermine effective responses when climate and pandemic crises collide to create a 'perfect storm'. The collision of climate extremes and pandemic control creates a type of compound event. The concept of 'compound event' was originally used in climatic research and defined as the 'combination of multiple drivers and/or hazards that contributes to societal or environmental risk' (AghaKouchak et al., 2020; Field, Barros, Stocker, & Dahe, 2012; Hao, AghaKouchak, & Phillips, 2013; Leonard et al., 2014; Zscheischler et al., 2018). Unable to foresee such a globally explosive outbreak of the coronavirus, those studies were mainly focused on the co-occurrence of multiple dependent climatic hazards. Only very recently have researchers begun to incorporate the coexistence of biological hazards. As the pandemic and global warming continues, civil society will see a growing probability of collisions between coronavirus surges and climate crises (Phillips et al., 2020), in tandem with other global issues, such as deglobalization, following recent trends. Countermeasures against one crisis may

[1] Locust swarms and climate change (unep.org)
[2] Federal Office of Meteorology and Climatology MeteoSwiss
[3] Trade Watch (worldbank.org)

jeopardize the effects against another and ultimately exacerbate the negative impacts of each crisis (Ishiwatari, Koike, Hiroki, Toda, & Katsube, 2020; Salas, Shultz, & Solomon, 2020; Selby & Kagawa, 2020). As a result, scholars have advocated for a comprehensive and holistic multi-hazard approach of disaster management that considers all possible hazards together with compound ones in the post-pandemic world (Chondol, Bhardwaj, Panda, & Gupta, 2020). Hariri-Ardebili (2020) proposed a multi-risk assessment tool to qualitatively study the hybrid impacts of compound-hazard situations on healthcare systems, while Shen, Cai, Yang, Anagnostou, and Li (2021) provided a tool to assess the compound risk from flooding and COVID-19 at the county level across the United States. Beyond these, researchers also developed optimization models to study the effectiveness of evacuation strategies in risk control when floods intersect with a pandemic (Pei, Dahl, Yamana, Licker, & Shaman, 2020; Shrabani, Udit, Mohit, Subhankar, & Subimal, 2021).

Another important aspect of risk management is to assess the economic consequences of hazardous events (Laframboise & Loko, 2012), however, this has been seldom touched upon so far in compound-hazard research. Typically, in single-hazard research, economic models, such as Input-Output (IO), Computable General Equilibrium (CGE) and agent-based hybrid models, provide quantitative tools to evaluate the economic footprint of disruptive events (Hallegatte, 2008; Miller & Blair, 2009; Okuyama & Santos, 2014; Rose, 1995, 2004). Metrics related to disaster-induced economic damages, both direct and indirect[4], are developed to inform cost-benefit decisions in disaster preparedness investment (ESCAP, 2019). With abundant studies focused on climate extremes (Hallegatte, 2014; Koks, Bockarjova, De Moel, & Aerts, 2015; Lenzen et al., 2019; Oosterhaven & Többen, 2017; Willner, Otto, & Levermann, 2018; Xia et al., 2018; Zeng, Guan, Steenge, Xia, & Mendoza-Tinoco, 2019), only a few have started studying biological hazards like the COVID-19 pandemic (Guan et al., 2020; McKibbin & Fernando, 2020). Even fewer studies have looked into the economic aspects of compound events. Zeng and Guan (2020) constructed an IO-based flood footprint model to quantify the combined indirect economic impacts resulting from multiple successive flood events. They concluded that the total economic impacts of a multi-flood event within a given region is usually larger than the sum of individual flood impacts, as the ensuing flood may disrupt the recovery of capital damaged by the first event. Similar perspectives are suggested in literature referring to the combination of a natural hazard and a pandemic. Sarkar-Swaisgood and Srivastava (2020) pointed out that the economic consequences of such compound events are underestimated if the interplay between individual hazards is not considered.

However, the interaction between the pandemic control and flood responses is different from that between two flood events. Flood events, the most common natural hazard globally, are usually sudden or rapid onset events which require immediate emergency measures (Bubeck, Otto, & Weichselgartner, 2017; Johnstone & Lence, 2009), while the pandemic lasts for longer periods and

[4] Direct damages refer to damages to humans, physical assets (e.g., buildings and infrastructure), and any other elements due to direct contact with disasters, relating directly in space and time to the disruptive event; while indirect damages are the subsequent losses induced by direct ones, including business interruption losses of affected economic sectors, the spread of losses towards other initially non-affected sectors, and the costs of recovery processes. They often occur, in space or time, after or outside the disaster event.

the corresponding control measures of various duration could coincide with different flood periods. A focus on measures to prevent coronavirus transmission can result in inadequate response towards flood disasters (Ishiwatari et al., 2020) and constrain the economic flows required by post-flood recovery, aggravating the impact of the flood. These differences in responses compared with the multi-flood situations increase the complexity of economic impact assessment, and thus an improved technique is needed to model the economic consequences of the intersection between natural and pandemic hazards.

Given the current research gap, we propose a compound-hazard approach to account for the economic impacts resulting from pandemic-induced perfect storms in this study. The confluence of the COVID-19 pandemic and flood disasters is selected as the focus of this study. The model, which is constructed under the agent-based ARIO framework (Hallegatte, 2008, 2014), considers not only the parallel threats of individual hazards on population and physical assets, but also examines the side effects of virus containment on post-flood recovery. We build multiple groups of scenarios where hypothetical hazardous events with different durations and intensities collide with each other at different spatial and temporal scales. We then use this approach to explore specific scenarios to understand the role of trade in disaster recovery during compound climate and health crises. In particular we look at how export restrictions and the extent of production specialization influence the magnitude of economic losses.

The model constructed in this research provides consistent and comparable loss metrics with single-hazard analysis and can be generalized to various types of compound events. This would support the formation of an integrated risk management strategy including compound hazards and the fulfillment of the mitigation and adaptation targets in the Paris Agreement and Sendai Framework for Disaster Risk Reduction (UNFCCC, 2015; UNISDR, 2015).

## 2. Methodology

The impact model for the pandemic-induced 'perfect storm' stems from the adaptive regional input-output (ARIO) model (Hallegatte, 2008, 2014), which is widely used in the realm of single-hazard analysis to simulate the propagation of negative shocks throughout the economy (Koks & Thissen, 2016; Okuyama & Santos, 2014). Compared with traditional IO and CGE models, the ARIO model is an agent-based model which provides the simplicity of IO modelling but also allows for some more flexibility than in CGE modelling (Oosterhaven & Bouwmeester, 2016). Recently Guan et al. (2020) proposed an extension of the ARIO model which considers cross-regional substitutability of suppliers to assess the global supply-chain effects of COVID-19 control measures. Drawing on that and in the context of compound hazards with pandemic control, the impact model constructed in this study improves the ARIO model in two ways. First, it combines the parallel shocks of natural and pandemic hazards on primary production inputs. Second, it considers the negative externality of pandemic control on the recovery of capital destructed by natural disasters. The collisions between flooding and pandemic control are taken as examples of compound events in this study.

Figure 1 presents the framework of our impact model, which is driven by compound-hazard input

variables and three modules, that is, a production module, an allocation module, and a demand module. The input variables refer to the initial shocks of flooding and pandemic control on production factors (i.e., labor and capital) respectively. The production module describes the firms' production activities under production and transport capacity constraints. The allocation module explains how the firms allocate output to their clients, including downstream firms and households, to satisfy the intermediate demand for inventory refilling and final demand for consumption and reconstruction. Finally, the demand module portrays how clients issue orders to their suppliers, which iterates into the next round of production until the economy recovers to the pre-disaster state.

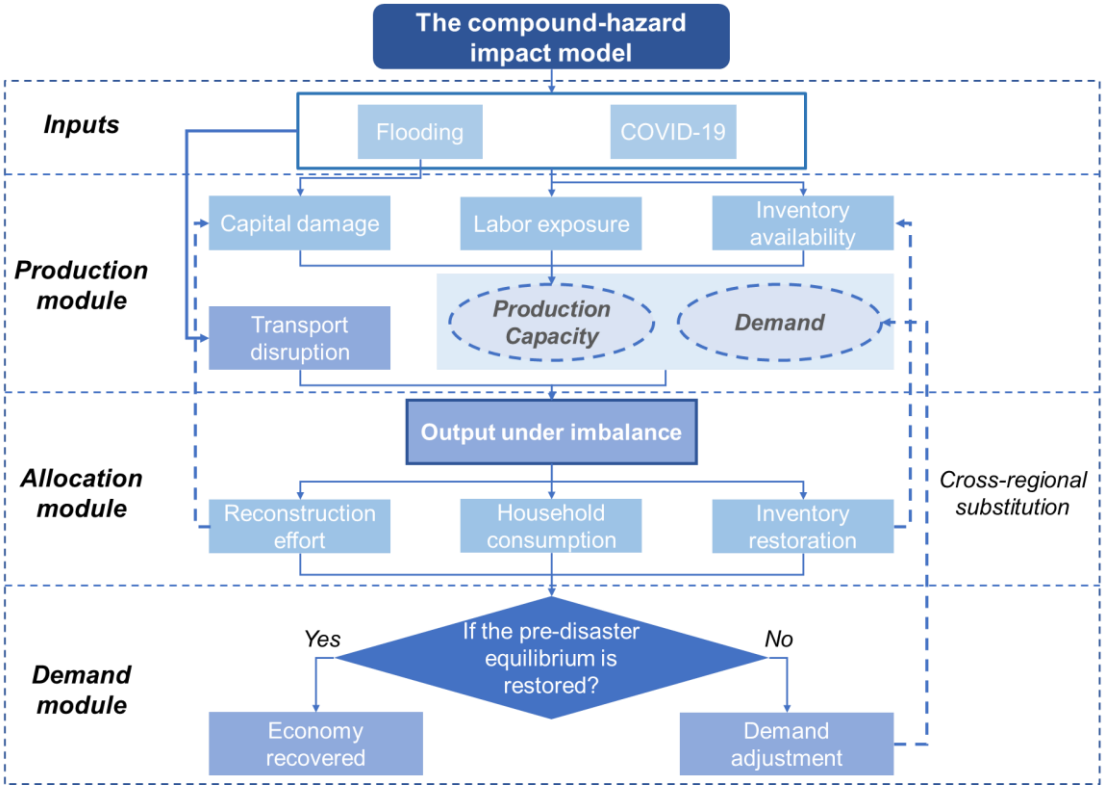


**Figure 1. Framework of the compound-hazard impact model.**

Our compound-hazard impact model starts with a closed multi-regional economy in equilibrium. A closed multi-regional economy excludes exchanges of goods and services (i.e., imports and exports) with external systems, while maintaining inter-regional flows within itself. A typical example of such economy is the global economy.

We define two types of economic agents, namely firms and households, distributed in $R$ regions within the economy. Firms make products which can be consumed by either downstream firms or households. There is a total of $P$ types of products, one-to-one corresponding to $P$ production sectors. Each firm produces a single product and belongs to a single sector. All the firms of a sector share the same production techniques, and therefore a firm can be completely substituted by another firm of the same sector from a different region. For simplification purposes, we adopt a representative firm to represent all the firms of a sector in a region, and there is a total of $N$

representative firms in the economy, where $N = R * P$. We also use a representative household which consumes multiple types of products to represent all the households in a region. The total number of representative households in the economy is equal to $R$.

Initially under the equilibrium conditions, the output of the representative firm of sector $i$ in region $r$, is equal to the aggregate demand for its products from both downstream firms and households over all regions. This is presented as follows:

$$\bar{x}_{ir} = \sum_{s=1}^{R} \sum_{j=1}^{P} a_{ir,js} * \bar{x}_{js} + \sum_{s=1}^{R} \overline{hd}_{ir,s} \ . \quad (1)$$

Here $\bar{x}_{ir}$ denotes the monetary value of the output of product $i$ in region $r$ in the equilibrium state. The first summation on the right-hand side of equation (1) represents the intermediate demand for product $i$ in region $r$ from downstream firms. $a_{ir,js}$ refers to the amount of product $i$ in region $r$ required to produce one unit of product $j$ in region $s$. This input coefficient is usually derived from the input-output matrix. The second summation calculates the final demand from households. $\overline{hd}_{ir,s}$ is the equilibrium quantity of product $i$ produced in region $r$ and consumed by the household in region $s$.

The above equilibrium breaks up following a pandemic-induced 'perfect storm', which triggers direct and knock-on effects on the whole economic system.

### 2.1 Compound exogenous shocks introduced by a 'perfect storm' to an economy system

The direct impacts of a 'perfect storm' on an economic system are multifaceted. The first category is the impact on production factors (e.g., productive capital and labor). The shortage or malfunction of production factors will reduce the firm's production capacity. The second category is the impact on infrastructure (e.g., transportation system). Transportation is critical for linking the supplies and demands of different agents in the economic networks. Transport failures will increase the inaccessibility to production materials and interrupt production activities. The third category is the impact on final demands. The adaptive behavior of consumers during or after the event will lead to structural changes of the final demands in the short term.

These three categories of direct impacts are not isolated. For example, the unavailability of transportation may lead to labor constraints. Restoring damaged productive capital will affect the structure of final d

emands in the disaster aftermath. These interactions between direct shocks introduced by a 'perfect storm' lead to complex indirect impacts on the economic system. Therefore, a systematic assessment method is needed to address these issues. We will analyze each type of the direct shocks and their

relations in detail in the following part of this section, and then introduce how to integrate these shocks into our compound-hazard impact model in section 2.2-2.4.

### 2.1.1 Capital damage

The amount of productive capital is reduced as physical assets, such as factories, machines, and equipment, are inundated by flooding and out of operation. We use $\gamma_{ir}^{K}(t)$ to denote the reduction in capital stock of sector $i$ in region $r$ in time step $t$, relative to the pre-disaster level, resulting from the perfect storm. It is calculated as:

$$\gamma_{ir}^{K}(t) = \gamma_{ir}^{K,F}(t) = \frac{\overline{K}_{ir} - K_{ir}(t)}{\overline{K}_{ir}}. \tag{2}$$

Here $\overline{K}_{ir}$ is the capital stock of sector $i$ in region $r$ in the pre-disaster equilibrium, and $K_{ir}(t)$ is the surviving capital stock of sector $i$ in region $r$ at time $t$. $\gamma_{ir}^{K,F}(t)$ refers to the proportion of capital damaged/destroyed by flooding alone. In this study we assume that the pandemic control has no direct impact on productive capital.

### 2.1.2 Labor damage

Labor damage induced by the 'perfect storm' is two-fold. First, , it increases the number of employees unable to work as a consequence of injury, illness or death from flooding or virus infection. Second, employees also spend less time working due to the damage to transport infrastructure and services during the event. Therefore, labor damage, $\gamma_{ir}^{L}(t)$, is expressed as the fraction of working hour loss in each sector and region during each time step, as below:

$$\gamma_{ir}^{L}(t) = \frac{\left[\overline{L}_{ir} - L_{ir}^{C}(t) - L_{ir}^{F}(t)\right] * \Delta wh_{ir}(t)}{\overline{L}_{ir} * \overline{wh}_{ir}}. \tag{3}$$

Here $\overline{L}_{ir}$ and $\overline{wh}_{ir}$ represents the number of employees and working hours per capita of sector $i$ in region $r$ at the pre-disaster levels. $L_{ir}^{C}(t)$ and $L_{ir}^{F}(t)$ are the numbers of workers unable to work due to virus infection and flooding at time $t$, respectively. $\Delta wh_{ir}(t)$ is the loss of working hours per capita in sector $i$ in region $r$ at time $t$. It is determined by the degree of transport disruption in region $r$, $\gamma_{r}^{Z}(t)$, as defined in the next section 2.1.3, and a sector-specific impact

multiplier, $\eta_i$ :

$$\Delta wh_{ir}(t) = \eta_i * \gamma_r^Z(t) * \overline{wh}_{ir} . \quad (4)$$

$\eta_i$ captures the impact of transport disruption on the operation of sector $i$ . It is based on three factors; the degree of exposure of the sector, for example, the extent of in-person interactions, whether it is the lifeline sector (electricity, for example) and the possibility for work at home (Guan et al., 2020). For example, the multiplier for the education sector could be low (e.g., 0.1) because of the development of online learning.

### 2.1.3 Transport disruption

The pandemic control and flooding have different but parallel impacts on the transportation system. For one thing, restrictions on public transport are placed in the epidemic regions to contain virus transmission. Those restrictions may include reducing the number of passengers to keep social distance and suspending international flights from epidemic areas. we use $\gamma_r^{Z,C}(t)$ to denote the strictness of the virus containment policy in region $r$ at the time step $t$ , which is measured by the percentage by which transportation capacity are reduced by lockdown measures relative to the equilibrium levels. For another, the transport infrastructure (e.g., roads, railways, and airports, etc.) could also be inundated and out of operation when the region is hit by a flood. We use $\gamma_r^{Z,F}(t)$ to represent the percentage of submerged transport infrastructure during flooding. Comparing these two aspects, we simply assume that the transport capacity from region $r$ to region $s$ is reduced by the larger one of the epidemic and flooding constraints in region $r$ , $\gamma_r^Z(t)$ . Therefore, the relative reduction of transport capacity from region $r$ to region $s$ at time $t$ , $\gamma_{r,s}^Z(t)$ , is calculated as below:

$$\gamma_{r,s}^Z(t) = \gamma_r^Z(t) = \max\left\{\gamma_r^{Z,C}(t), \gamma_r^{Z,F}(t)\right\} . \quad (5)$$

The reduction in transport capacity between regions has two-fold impacts on the economic system. First, it affects labour supply, which has been discussed in the previous section 2.1.2. Second, it increases the difficulty in delivering the intermediate products for the next round of production and the final products for household consumption to the downstream producers and consumers. Similar with the labour constraint, we define the connectivity loss between sectors from different regions as below:

$$\gamma^{Z}_{ir,js}(t) = \eta_i * \gamma^{Z}_{r,s}(t) \tag{6}$$

Here the connectivity loss, $\gamma^{Z}_{ir,js}(t)$, is expressed by the relative reduction in the capacity to transport the product of sector $i$ in region $r$ to sector $j$ in region $s$ at time $t$.

### 2.1.4 Final demand shock

Finally, households adjust their consumption in response to the perfect storm. For example, they spend more time in staying at home and less money on eating out, hotels and other outdoor entertainment. Households in disasters also show a propensity for stocking medical and rescue products, such as masks and life jackets. Here we simply assume that the local consumption, import and export of the accommodation, food and recreation services decline by $\alpha$ % in the epidemic and flooded regions, while the local consumption and import of medical services and emergency products increase by $\beta$ % in these regions. This adaptive behaviour of households is expressed as below:

$$hd_{ir,s}(t) = (1-\alpha\%)^{I(i\in\Omega_\alpha)*I(r,s\in R_C\cup R_F)} * (1+\beta\%)^{I(i\in\Omega_\beta)*I(s\in R_C\cup R_F)} * \overline{hd}_{ir,s}. \tag{7}$$

Here $hd_{ir,s}(t)$ refers to the consumption of the household in region $s$ for product $i$ in region $r$ at time $t$. $I(i\in\Omega_\alpha)$ is the indicator function which takes value 1 when product $i$ belongs to the sector set of accommodation, food, and recreation services ($\Omega_\alpha$). Otherwise, it takes value 0. $I(r,s\in R_C\cup R_F)$ is the indicator function which takes value 1 when region $r$ or $s$ is one of the epidemic regions ($R_C$) or flooded regions ($R_F$). Similarly, $I(i\in\Omega_\beta)$ is the indicator function which takes value 1 when product $i$ belongs to the sector set of medical services and emergency products ($\Omega_\beta$). $I(s\in R_C\cup R_F)$ is the indicator function which takes value 1 when region $s$ is one of the epidemic or flooded regions.

## 2.2 Production under compound constraints

The representative firms in the economy rent capital and employ labour to process natural resources and intermediate inputs produced by other firms into a specific product. The production process of the firm in sector $i$ and region $r$ is defined as below:

$$x_{ir} = \min\left\{\frac{z_{j,ir}}{a_{j,ir}}; \frac{va_{k,ir}}{b_{k,ir}}\right\}, \quad j = 1,...,P, \quad k = 1,2\,. \tag{8}$$

Here $x_{ir}$ demotes the output of the firm in sector $i$ in region $r$ in monetary values. $z_{j,ir}$ are the intermediate products of sector $j$ in region $s$ used in the production process of the firm in sector $i$ in region $r$. $va_{k,ir}$ are the value-added/primary inputs (i.e., capital and labour in this study) used by this firm. $a_{j,ir}$ and $b_{k,ir}$ are the input coefficients calculated as below:

$$a_{j,ir} = \frac{\bar{z}_{i,ir}}{\bar{x}_{ir}}, \tag{9}$$

and

$$b_{k,ir} = \frac{\overline{va}_{k,ir}}{\bar{x}_{ir}}. \tag{10}$$

Here the overbar indicates the value of that variable in the equilibrium state. Therefore $a_{j,ir}$ and $b_{k,ir}$ stand for the amount of intermediate product $j$ and primary input $k$, that is, capital or labour, required to produced one unit of product $i$ in region $r$.

Equation (8) follows the form of the Leontief production function, which is commonly used in short-term impact analysis (Miller & Blair, 2009). It does not allow substitution between different types of inputs, as economic agents do not have enough time to adjust other inputs to replace temporary shortages. However, we still allow for the substitution between products of the same sector from different regions. As in Equation (8)-(10), we do not distinguish between intermediate product $j$ from different regions, as we consider that products of the same sector from different regions are completely mutual complementary.

**2.3 Demand and resource allocation system during in-equilibrium period**

Demand in the disaster aftermath can be categorized into three strands, i.e., intermediate demand, final demand, and recovery demand. Products made under constraints induced by disasters will flow to these demands on the market. During an in-equilibrium period, probably not all demands can be met by outputs. We use a proportional rationing scheme to model the resource allocation process during an in-equilibrium period.

### 2.3.1 Intermediate demand

Firm orders its supplier because of the need to restore its intermediate product inventory. We assume that each firm has a specific target inventory level based on its maximum supply capacity in each time step,

$$S_i^{p,*}(t) = n_i^p * a_i^p * x_i^{max}(t)$$

Then the order issued by firm $i$ to its supplier $j$ is

$$FOD_j^i(t) = \begin{cases} \left(S_i^{p,*}(t) - S_i^p(t)\right) * \dfrac{\overline{FOD}_j^i * x_j^a(t)}{\sum_{j \to p}\left(\overline{FOD}_j^i * x_j^a(t)\right)}, & \text{if } S_i^{p,*}(t) > S_i^p(t); \\ 0 & \text{if } S_i^{p,*}(t) \le S_i^p(t). \end{cases}$$

### 2.3.2 Final demand

Households issue orders to their suppliers based on their demand and the supply capacity of their suppliers. In this study, the demand of household $h$ to final products $q$, $HD_h^q(t)$, is given exogenously at each time step. Then, the order issued by household $h$ to its supplier $j$ is

$$HOD_j^h(t) = HD_h^q(t) * \frac{\overline{HOD}_j^h * x_j^a(t)}{\sum_{j \to q}\left(\overline{HOD}_j^h * x_j^a(t)\right)}$$

### 2.3.3 Resource allocation system

By adding up all orders received, the total order received by firm $j$ is

$$TOD_j(t) = \sum\nolimits_i FOD_j^i(t) + \sum\nolimits_h HOD_j^h(t)$$

The allocation module mainly describes how suppliers allocate products to their clients. When some firms in the economic system suffer a negative shock, their production will be constrained by a shortage to primary inputs such as a shortage of labour supply in the outbreak of COVID-19. In this case, a firm's output will not be able to fill all orders of its clients. A *rationing scheme* that reflects a mechanism based on which a firm allocates an insufficient amount of products to its clients is needed (Bénassy, 1993; Wenz & Levermann, 2016). For this case study, we applied a *proportional* rationing scheme according to which a firm allocates its output in proportion to its orders. Under the proportional rationing scheme, the amounts of products of firm $i$ allocated to firm $j$ and household $h$ is as follows,

$$FRC_j^i(t) = \frac{FOD_i^j(t-1)}{\left(\sum_j FOD_i^j(t-1) + \sum_h HOD_i^h(t-1)\right)} * x_i^a(t)$$

$$HRC_h^i(t) = \frac{HOD_i^h(t-1)}{\left(\sum_j FOD_i^j(t-1) + \sum_h HOD_i^h(t-1)\right)} * x_i^a(t)$$

Firm $j$ received intermediates to restore its inventories,

$$S_j^{p,restored}(t) = \sum_{i \to p} FRC_j^i(t)$$

Therefore, the amount of intermediate $p$ held by firm $i$ at the end of period $t$ is as below:

$$S_j^p(t) = S_j^p(t-1) - S_j^{p,used}(t) + S_j^{p,restored}$$

### 2.4 The footprint of a 'perfect storm'

The economy will recover to the pre-crisis equilibrium after all constraints are lifted, i.e., all destroyed/damaged productive capital are recovered, all labor constraints are lifted, and all business linkages are repaired. We define the value-added decrease of each industrial sector in an economy caused by compound exogenous shocks as the economic impacts of the 'perfect storm'. The impact of the initial exogenous shock continuously propagation on the economic network, from one sector to another and one region to another, leaving a footprint in the network. We use the concept, disaster footprint, as a vivid expression of the overall economic impact of a 'perfect storm'. The *footprint* of a 'perfect storm' is calculated as

$$Footprint = \sum_{s,j} \left( \sum_u va_{u,s,j,0} \times T - \sum_{u,t} va_{u,s,j,t} \right)$$

where $T$ represents the total periods used to recovery to the pre-disaster equilibrium.

## 3. Data: a hypothetical global economy

We apply our compound-hazard impact model to a hypothetical global economy to examine its applicability in assessing the economic footprint of a perfect storm of climate extremes and pandemic control. This hypothetical global economy consists of four regions and five sectors. Table S1 in the Appendix represents the transactions between these regions and sectors, which are extracted from the multiregional Input-Output table developed by Zheng et al. (2020). We mark the four regions by region A, region B, region C and region D. Among them region C is the only region

that is hit by flooding, while the pandemic control could take place in any one of the four regions. Region B has the closest trade relationship with region C. The trade volume between region B and C reaches 10.6% of region C's output, followed by region A (6.2%) and D (3.5%). The five sectors include Agriculture (AGR), General Manufacturing (MANG), Capital Manufacturing (MANR), Construction (CON) and Other Services (OTH). 'MANR' and 'CON' are the two sectors that are involved in reconstruction of capital damaged by flooding. We assume that capital reconstruction largely relies on local inputs of capital goods and construction services. For example, the 'CON' and 'MANR' sector of region C contribute to 68% and 20% of the reconstruction efforts in region C, respectively, while the remaining 12% comes from the 'MANR' and 'CON' sectors of region B and the 'MANR' sector of region A. A full capital matrix indicating the sources of capital formation of each region is provided in Table S2 in the Appendix. The model is run on a weekly basis in this study.

## 4. Scenarios and Results

### 4.1 Multi-scale floods collide with pandemic control in different spatial spreads

***Key findings:*** *The total economic losses across all regions, relative to annual global GDP, increase with the spatial expansion of the pandemic control, regardless of the flood scales. Among all the 'perfect storm' settings, the flooded region suffers the least GVA losses when the pandemic control occurs outside itself, still exacerbating the single-flood impact by 0.15%-0.97% according to flood scales. Some non-flooded regions closely economically connected with the flooded region benefit from the stimulus effects from the reconstruction demand which grows with flood scales.*

In this section, our compound-hazard impact model is used to simulate the a group of scenarios, when multi-scale floods intersect with pandemic control on different spatial scales. Three scales of floods are defined according to the severity of damages they cause directly to population and economic sectors (see Table 1). All floods occur in week 5 and last for 2 weeks in region C. For example, a small flood is defined to affect 20% of the population in C, a medium flood affects 40% of its population, and a large flood affects 60%.

**Table 1. Direct damages caused by small, medium, and large flooding.**

| Flood scales | Direct damage (in relative terms) | | | | | |
|---|---|---|---|---|---|---|
| | Population | Agriculture | Manufacture, general | Manufacture, capital | Construction | Services |
| **Small** | 0.2 | 0.2 | 0.1 | 0.1 | 0.15 | 0.15 |
| **Medium** | 0.4 | 0.4 | 0.2 | 0.2 | 0.3 | 0.3 |
| **Large** | 0.6 | 0.6 | 0.3 | 0.3 | 0.45 | 0.45 |

At the same time as the flooding occurs, we assume that regions affected by the pandemic begin to

take measures to bring its spread under control. The strictness of the control policy is benchmarked at 30% for 24 weeks. Four scenarios of pandemic control are designed according to the spatial spread of the outbreak: a) No pandemic control; b) Pandemic control in region C; c) Pandemic control in region A, B, and D; d) Pandemic control over all regions.

Figure 2 presents the weekly changes of regional gross value-added (GVA), relative to the pre-disaster level, in the four regions under different combinations of flooding and pandemic control scenarios. Numbers in each plot indicate the cumulative losses or gains of regional GVAs over time, relative to the annual global GDP. From left to right, each column represents the small-, medium-, and large-scale flooding in region C. From top to bottom, each row stands for one of the four pandemic control scenarios listed above.

As shown in the first row, when there is no pandemic control, the accumulative relative losses in region C, which is the only flooded region and in yellow lines, increase from 0.57% (small flood), to 1.68% (medium flood) and finally to 3.27% (large flood). Region D also experiences increasing losses in its GVA, although very tiny, attributable to the spill-over effects along the supply chain across regions. By contrast, the other two non-flooded regions, A and B, witness slight growth in their GVAs. This comes from the stimulus effect of reconstruction activities to recover capital damaged by flooding. When substitution of suppliers is allowed, such stimulus effect is stronger in non-flooded regions with which the flooded region closely trades (Koks & Thissen, 2016). When region C is flooded and unable to meet the increasing demand for reconstruction, clients will choose suppliers in region A and B to restore their damaged capital, which stimulates the economic performance there. Among all regions, B benefits most from flooding in C, as it is the region that has the closest economic relationship with C. Furthermore, this stimulus effect expands with the flood scales in C. For example, the gains in GVA for region B is 0.07% from a small flood in C. This figure rises to 0.25% in medium flooding and further to 0.37% in large flooding.

Comparing the bottom three rows with the first row, we find that the total losses in the four regions increase with the spatial expansion of the pandemic control, regardless of the flood scales. Given the medium flood scenario (the second column), when there is no pandemic control as in the first row, the total GVA of the four regions drops by 1.38%. This figure increases to 3.60% when a 30%-24-week pandemic control policy is implemented in region C simultaneously with flooding. It then jumps to 11.18% when the pandemic control takes place in all the non-flooded regions as well as C. The rapid growth in the total losses is ascribed to the difficulty in finding a replacement of suppliers when all regions are affected by either flooding or pandemic control. Finally, the total relative losses increase by another 1.46% when the pandemic control expands to all regions.

Looking at regional details, we find that regions that originally benefit from flooding in C start to bear GVA losses when the spread of the pandemic control is wide enough or the flood is small enough. Region A begins to have GVA losses (0.04%) when a small flood intersects with a pandemic control over C, while region B does not have GVA losses until the pandemic control spreads to all the non-flooded regions. In addition, when the pandemic control occurs (among the bottom three rows), region C suffers the least economic losses when the control is held outside itself (the third

row). For example, in the large flood scenarios (third column), the GVA losses in region C is 4.24% in the third row, smaller than 4.72% in the second row and 5.15% in the fourth row, but still larger than 3.27% in the first row where there is no pandemic control. The increment of losses from 3.27% to 4.24%, of 0.97%, indicates the level of side effects which pandemic control outside of region C imposes on the post-flood recovery within that region. On the other hand, for regions A, B and D, the biggest GVA losses are found in the third row of the first column when a small flood collides with pandemic control over all the non-flooded regions. In this scenario, these regions are not only directly affected by the pandemic control, which makes them less capable to replace production in region C, but also benefit less from the reconstruction demand and the accompanying stimulus effect arising from a smaller flood.

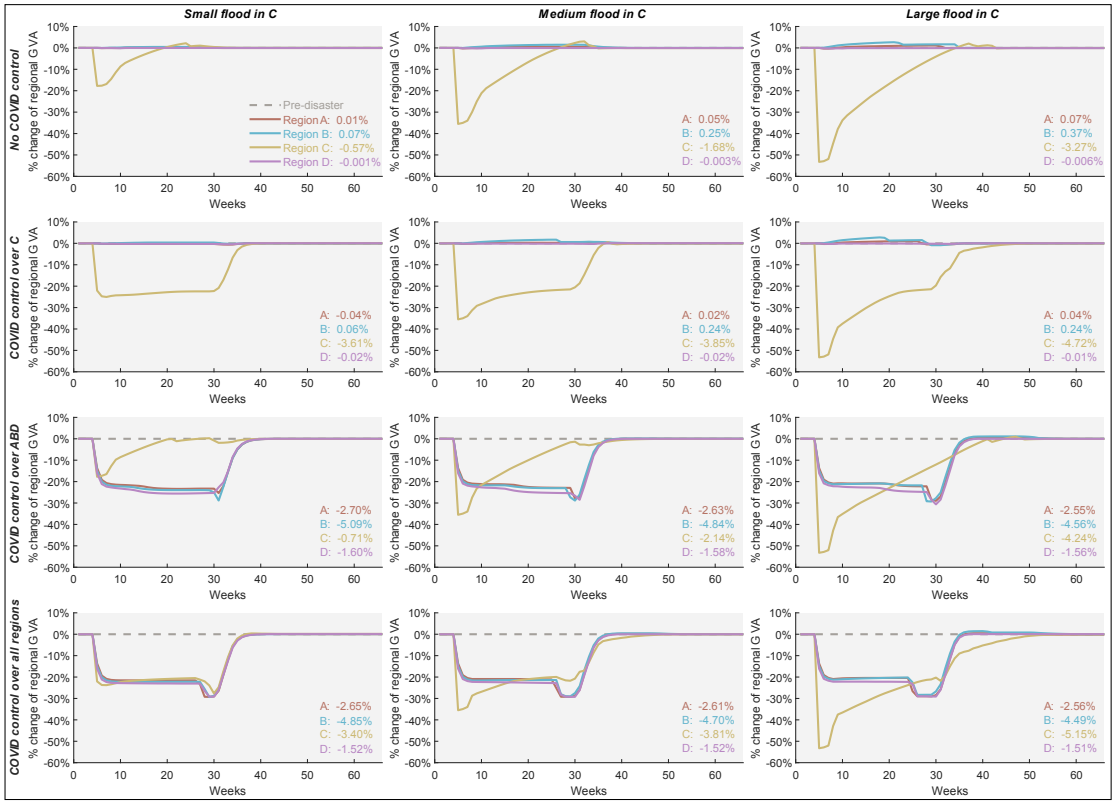


**Figure 2. Weekly changes of regional GVAs, relative to the pre-disaster levels, in four regions, when multi-scale floods collide with pandemic control on different spatial scales.** The numbers in each plot indicate the accumulative losses (negative ones) or gains (positive ones) of regional GVAs over time, relative to the annual global GDP. From left to right, each column represents the small-, medium-, and large-scale flooding in region C. From top to bottom, each row stands for one of the four pandemic control scenarios: a) No pandemic control; b) Pandemic control in region C; c) Pandemic control in region A, B, and D; d) Pandemic control over all regions.

### 4.2 Multi-scale floods collide with different strictness of pandemic control

***Key findings:*** *The total economic losses in the four regions, relative to annual global GDP, increase with the strictness of the pandemic control, irrespective of the flood scales. The post-flood reconstruction to some extent offsets the negative impacts of the 'perfect storm'. Regions with the strictest pandemic control benefit from other regions increasing their strictness given the cross-regional substitutability.*

In this section, we set up a second group of scenarios, where multi-scale floods collide with different strictness of the pandemic control. The three scales of floods are designed as in section 3.1 (see Table 1). The pandemic control starts at the same time with the flood over all regions and lasts for 24 weeks. Figure 3 presents the weekly changes of regional GVAs relative to the pre-disaster levels when small-, medium- and large-scale floods collide with pandemic control at: a) 10% strictness for all regions; b) 10% strictness for region A and C, 50% strictness for region B and D; c) 50% strictness for all regions.

On the global scale, the total economic losses in the four regions increase with the strictness of the pandemic control, irrespective of flood scales. Comparing each row, the total GVA losses in the four regions is 3.94% (small flood), 4.46% (medium flood) and 5.67% (large flood) when the pandemic control is at 10% strictness for all regions (the first row). These figures climb to 15.22%, 16.07% and 17.99%, respectively, when the strictness of the pandemic control goes up to 50% but only in regions B and D (the second row). They culminate in losses of 22.90%, 22.95% and 23.48%, respectively, when 50% pandemic control is enforced in all regions (the third row). The total losses also increase with flood scales in all these pandemic control scenarios.

On the regional scale, the cumulative GVA losses in region C grow with both the scale of the flood and the strictness of the pandemic control, similar with the trend of the global losses described above. Specifically, its losses rise from 1.21% in the upper left to 7.33% in the bottom right. By comparison, the cumulative losses in region A increase with the strictness of the pandemic control but decrease with the scale of the flood. The smallest losses in region A are found in the upper right plot at 0.65%, while the biggest losses lie in the bottom left at 4.88%. Given the strictness of the pandemic control, region A endures less economic losses from a larger flood in C, as a result of stronger stimulus effect from larger reconstruction demand. Similar trends regarding flood scales are observed in losses of non-flooded regions B and D and suffer less than A from a larger flood in C. Here, a general conclusion can be drawn that while the pandemic control increases the economic losses from flooding, the post-flood reconstruction and substitution effects to some extent offset the negative impacts. Furthermore, for region B and D, the greatest GVA losses occur when they go through stricter pandemic control than other regions, that is, the pandemic control scenario defined in the second row in Figure 3. Taking the small flood as an example (first column), the GVA losses in region B and D reach as much as 9.52% and 2.91% in the second row, even larger than 8.91% and 2.74% respectively during the globally strictest pandemic control (i.e., 50% for all regions in the third row). The reason is that in the second-row scenario, some economic activities are substituted

from regions B and D to regions A and C when the latter regionsare less restricted by the pandemic control measures. Therefore, we can conclude that the losses for regions with the strictest pandemic control are reduced when other regions increase the strictness of their pandemic control given the cross-regional substitutability.

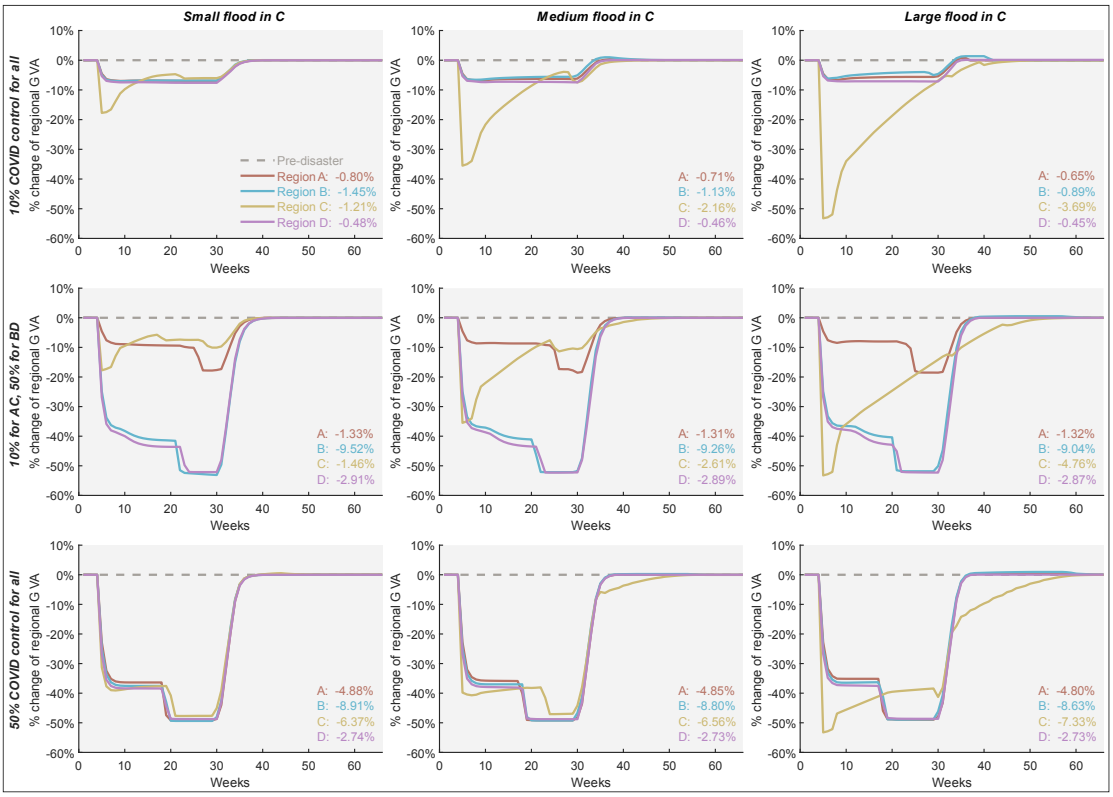


**Figure 3. Weekly changes of regional GVAs, relative to the pre-disaster levels, in four regions, when multi-scale floods collide with different strictness of pandemic control.** The numbers in each plot indicate the accumulative losses (negative ones) or gains (positive ones) of regional GVAs over time, relative to the annual global GDP. From left to right, each column represents the small-, medium-, and large-scale flooding in region C. From top to bottom, each row stands for one of the three pandemic control scenarios: a) 10% strictness of pandemic control over all regions; b) 10% control for region A and C, 50% control for region B and D; c) 50% strictness of pandemic control over all regions.

### 4.3 Multi-scale floods collide with intermittent pandemic control in different flood periods

***Key findings:*** *Slightly more economic losses are expected when the pandemic control occurs after flooding than before flooding. Shorter duration and higher strictness of pandemic control would result in less economic losses in all regions, regardless of the flood scales.*

In this section, we investigate a third group of scenarios, where intermittent pandemic control occurs across different flood periods. Like the previous two groups, the flood may be small, medium or

large, as defined in Table 1. The flood hits region C in week 10 and lasts for 2 weeks. Then we assume three different pandemic control scenarios: 1) 30%-24 week pandemic control that starts 7 weeks before flooding; b) 30%-24 week pandemic control that starts 15 weeks after flooding; c) 60%-8 week pandemic control that commences 15 weeks after flooding. Here, all the pandemic control scenarios occur in all regions.

Comparing the first two rows of Figure 4, slightly more economic losses are expected when the pandemic control occurs after flooding. Given a large flood in C (the third column), the cumulative GVA losses in region A is 2.56% when the pandemic control takes place before flooding (the first row). This figure rises to 2.63% when the control occurs after flooding (the second row). Similar increases can be seen in all other regions. A possible reason is that subsequent pandemic control has long-lasting impacts on flood-induced reconstruction activities. Particularly for region C (in yellow lines), it is obvious that the post-flood economic recovery is hampered by the pandemic control from week 25.

Comparing the bottom two rows of Figure 4, we find that a combination of shorter duration and higher strictness of pandemic control would result in less economic losses in all regions, regardless of the flood scales. The total GVA losses in the four regions are 13.20% when a 30%-24 week pandemic control interfaces with the recovery period from a small flood (second row and first column). This figure falls to 10.69% when the strictness-duration combination of the control becomes 60%-8 weeks (third row and first column). Similar results are found for the medium and large flood scenarios. This is consistent with the results of Guan et al. (2020) who studied the global economic costs of COVID-19 control measures in a single-hazard setting. Therefore, an important insight here is that a stricter pandemic control policy for a shorter duration results in lower economic costs when battling both flooding and a pandemic.

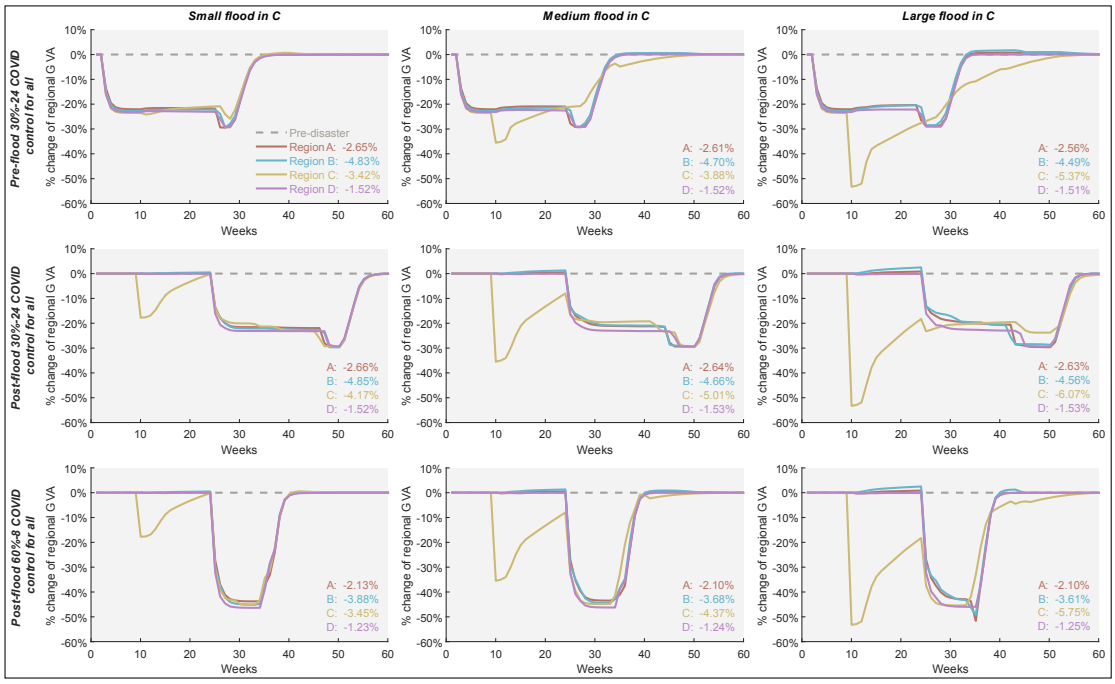

**Figure 4. Weekly changes of regional GVAs, relative to the pre-disaster levels, in four regions, when multi-scale floods collide with pandemic control intermitting in different flood periods.** The numbers in each plot indicate the accumulative losses (negative ones) or gains (positive ones) of regional GVAs over time, relative to the annual global GDP. From left to right, each column represents the small-, medium-, and large-scale flooding in region C. From top to bottom, each row stands for one of the three pandemic control scenarios: a) 30%-24 control occurring 7 weeks before flooding; b) 30%-24 control occurring 15 weeks after flooding; c) 60%-8 control occurring 15 weeks after flooding.

### 4.4 Multi-scale floods collide with pandemic control and export restrictions

***Key findings:*** *Export restrictions increase the economic losses during the collision of flooding and pandemic control.. These losses increase non-linearly with the size of the trade restrictions. While all regions suffer from export restrictions, those that depend more on regional trade are more vulnerable to a universal export restriction.*

Previous scenarios are built on a 'free trade' economy where goods and services flow across regions without any barriers. However, global shocks such as the pandemic increase pressures towards deglobalization including through the imposition of measures such as export restrictions on critical goods, such as medical products and food (Espitia, Rocha, & Ruta, 2020).

In this section, we simulate the economic impacts of a 'perfect storm' of flooding, pandemic, and deglobalization. We assume a 25%, 50% or 75% export restriction on all goods and services for all regions. The export restriction is applied in parallel with the pandemic control, which is benchmarked at 30% strictness for 24 weeks over all regions. These measures occur at the same time as the flooding.

Figure 5 shows the weekly changes in GVAs of the four regions, relative to the pre-disaster levels, under different combinations of flood scales and export restrictions. Compared to the 'free trade' scenario (the bottom row in Figure 2), a 25% export restriction increases the total economic losses by 1.81%, 1.72%, and 1.91%, relative to the annual global GDP, when a small, medium, and large flood intersects with the benchmark pandemic control, respectively; while a 50% export restriction adds another 2.18%, 2.07%, and 2.10% to the total losses, respectively, compared to the 25% export restriction; finally, a 75% export restriction adds another 2.62%, 2.62%, and 2.36% to the total losses, respectively, compared to the 50% export restriction. The total economic losses over all regions increase non-linearly with the degree of export restriction. Stronger export restrictions bring about larger increments in economic losses than weaker ones.

At the regional level, Figure 5 shows that region A (brown line) and D (purple line) are more vulnerable to the escalating export restriction than other regions. For example, the cumulative GVA losses in region A grow by 0.63%, 1.33% and 2.09%, relative to the annual global GDP, when the export restriction increases from 0% to 25%, 50%, and 75%, respectively, during the

confluence of an average flood and the benchmark pandemic control. By comparison, region B (blue line) is the least sensitive to the export restriction, but still suffers considerable extra losses. This may be partly related to the different degrees of trade dependence of the regional economies. Specifically, for regions A and D, their trades with other regions account for around 30% and 31% of their total output, respectively, which are higher than for the other two regions (23% for B and 20% for C). Higher dependence on inter-regional trade increases economic vulnerability when countries impose trade restrictions.

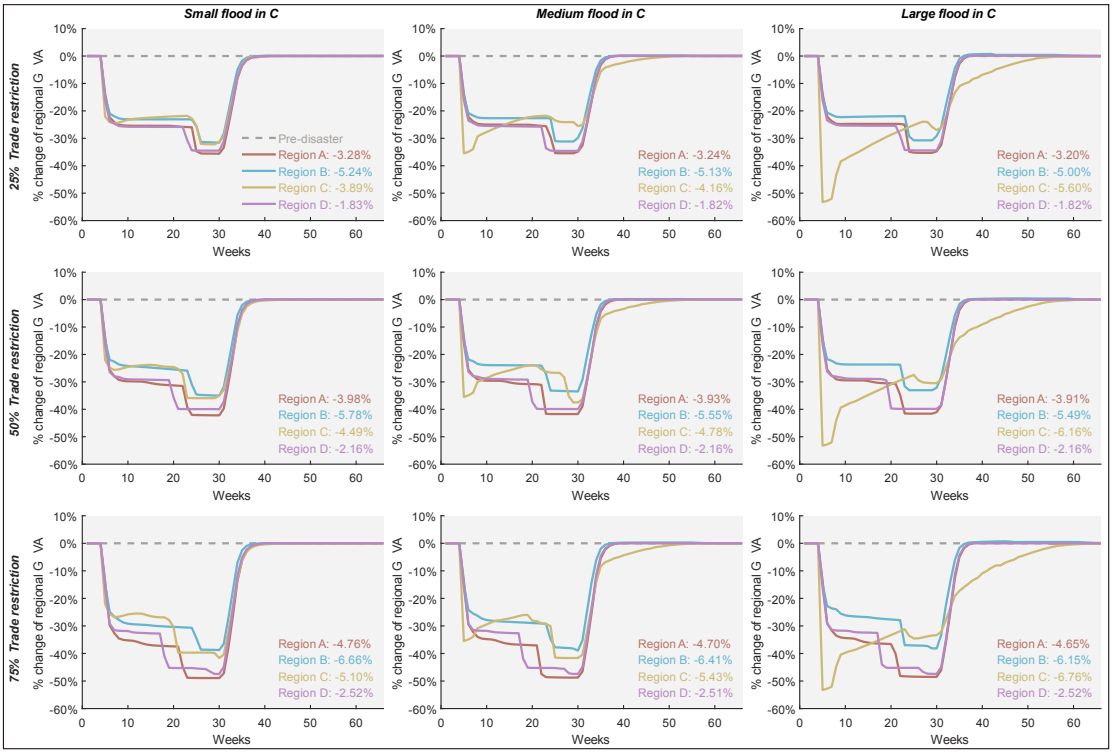


**Figure 5. Weekly changes of regional GVAs, relative to the pre-disaster levels, in four regions, when multi-scale floods collide with pandemic control and export restrictions.** The numbers in each plot indicate the accumulative losses (negative ones) or gains (positive ones) of regional GVAs over time, relative to the annual global GDP. From left to right, each column represents the small-, medium-, and large-scale flooding in region C. From top to bottom, each row stands for 25%, 50% and 75% export restrictions on all goods and services over all regions.

### 4.5 Multi-scale floods collide with pandemic control and specialized production

***Key findings:*** *Specialization, particularly of economically key-node sectors, aggravates the economic impacts of a 'perfect storm' of flooding, pandemic control and trade restrictions. Such impacts are more than doubled by the imposition of a 50% export restriction on those specialized sectors.*

Cross-regional substitutability of suppliers is a key assumption in the compound-hazard impact

model which enhances the resilience of the economic network against the 'perfect storm'. The substitution between products of the same sector from different regions is quite common in most cases. For example, a general consumer would not care much whether his Nike shoes are made in Vietnam or China, or a brewery may use barley from Germany or the Czech Republic. However, some products are less substitutable. For example, some Chinese herbs are only planted in China for medical treatment and cannot be substituted elsewhere. Meanwhile, in the automotive sector, some unique parts of a popular car model, such as Tesla Model X, are usually provided by a specialized supplier with little substitutability.[5]

Specialization in production reduces the substitutability of products, and this section is targeted to examine its impacts on economic resilience during a 'perfect storm'. We make three sectors in different regions produce specialized products which cannot be substituted elsewhere. Among them are the agriculture sector in region D (denoted by 'Agr-D'), the capital manufacturing sector[6] in region B ('Manr-B') and the general manufacturing sector in region C ('Mang-C'). We select these three sectors for a purpose, as the latter two sectors are two important nodes in the economic network in terms of having large trade volumes with other sectors. Specifically, trade flows from and to the 'Mang-C' and 'Manr-B' sectors reach 9.1% and 8.2% of the global GDP, respectively, ranking as second and third among all sectors. By contrast, the 'Agr-D' sector is among those with the least traded inputs and outputs (0.6%). We explore the economic impacts when the exports of these specialized sectors are restricted by 50% during the collision of a flood and a pandemic control. The flood strikes region C for 2 weeks with three possible scales, as defined in Table 1, and the pandemic control is benchmarked at 30% strictness for 24 weeks over all regions.

Figure 6 presents the weekly changes in GVAs of the four regions, relative to the pre-disaster levels, under different combinations of flood scales and specialization scenarios. Comparing the first row of Figure 6 and the bottom row of Figure 2 (baseline scenario), the specialization of the agricultural sector in region D does not exacerbate the economic impacts until the flood scale grows large. During the intersection of a pandemic control and a large flood in C (third column), almost all the additional losses caused by specialization of the 'Agr-D' sector are found in region D, whose losses increase marginally from 1.51% to 1.53%, relative to the annual global GDP, compared to the baseline scenario.

In comparison, the greater specialization of some key node sectors of the economic network increases the vulnerability of the economy against the 'perfect storm'. In the second row of Figure 6, when there are limited substitution possibilities away from the capital manufacturing sector of region B and the general manufacturing sector of region C due to specialization, the total economic

---

[5] Boehm et al (2019) examine the impact of the Japanese earthquake and find that in the US, exposure to the shock is very much concentrated among affiliates of Japanese multinationals relative to non-Japanese firms. For these exposed firms, a proxy for output declines in almost the same proportion as the decline in imported intermediate inputs from Japan and this is driven by changes in the quantity of imports rather than through changes in dollar denominated prices. This suggests that affiliates of Japanese firms in the US were unable to quickly substitute alternative inputs in the short run.

[6] The capital manufacturing sector is the sector which produces capital goods involved in the reconstruction process.

losses of the four regions rise by 0.02% (small flood), 0.14% (medium flood), and 0.92% (large flood), respectively, compared to the baseline scenario. Among the four regions, region B undergoes the greatest increase in GVA losses, followed by region A and D, while region C has the least increase. For example, given the large flood in C (third column), specialization of the three sectors inflicts region B with extra losses amounting to 0.51%, nearly twice that of region A (0.26%) and four times that of region D (0.13%).

Finally, devastating impacts occur with the imposition export restriction with specialized production. Comparing the third row of Figure 6 and the baseline scenario, when a 50% export restriction is imposed, the total GVA losses of the four regions reach as much as 28.83% (small flood), 29.30% (medium flood) and 30.67% (large flood), respectively, relative to the annual global GDP, more than double the impacts under the baseline scenario (12.43%, 12.64% and 13.71% with small, medium, and large floods). This time, region B still suffers the biggest increase in GVA losses, but followed by region C and A, with region D experiencing the least increase.

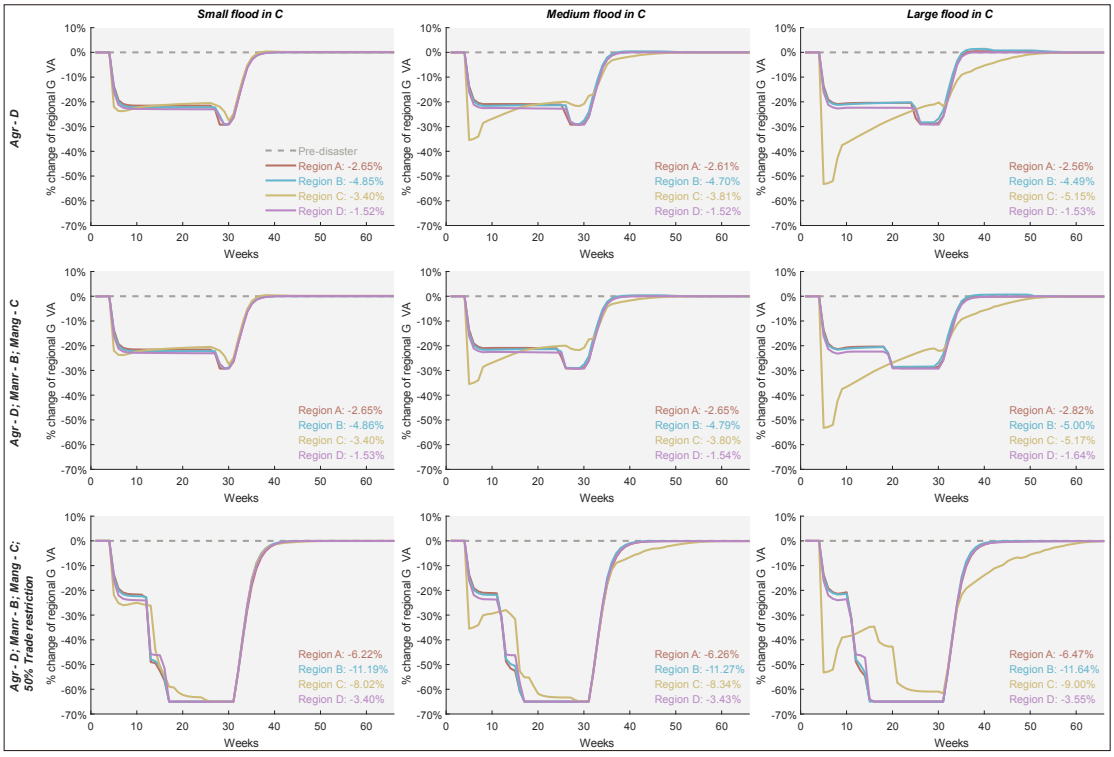


**Figure 6. Weekly changes of regional GVAs, relative to the pre-disaster levels, in four regions, when multi-scale floods collide with pandemic control and specialized production.** The numbers in each plot indicate the accumulative losses (negative ones) or gains (positive ones) of regional GVAs over time, relative to the annual global GDP. From left to right, each column represents the small-, medium-, and large-scale flooding in region C. From top to bottom, each row stands for one of the three specialization scenarios: a) specialization only happens in the agriculture sector of region D ('Agr-D'); b) specialization occurs in the agriculture sector of region D, the capital manufacturing sector of region B ('Manr-B'), and the general manufacturing sector of region C ('Mang-C'); c) the above three specialized sectors are also imposed by a 50%

export restriction.

## 5. Discussion and conclusion

In this study, we construct a compound-hazard impact model to simulate the economic footprint of a pandemic-induced perfect storm, taking the collision of flooding, pandemic control and export restrictions as an example. Our compound-hazard impact model improves the standard ARIO model, which is commonly used in single-hazard impact analysis, by considering the interplay between different types of hazardous events for the first time. We also incorporate the possibility of substitution between suppliers of the same sector from different regions, which could lead to higher resilience of the economic network against a perfect storm and lower estimates of economic consequences. We build five groups of scenario sets to test the robustness of our model on a hypothetical global economy of 4 regions and 5 sectors. These scenarios are designed to investigate how the economic impacts of the perfect storm react to 1) the spatial spread of the pandemic; 2) the strictness of the pandemic; 3) the occurrence time of the pandemic; 4) the imposition of a universal export restriction; and 5) the presence of specialized production. The latter two special scenarios sets are included here as a reflection on the ongoing deglobalization.

Several conclusions can be drawn from the simulation results. First, the concurrence of pandemic control during a single-flood event hampers the post-flood recovery and engenders extra economic losses. This confirms the idea from an economic perspective that restrictions targeted at coronavirus containment results in inadequate flood responses, aggravating the flood impacts (Ishiwatari et al., 2020; Sarkar-Swaisgood & Srivastava, 2020; Selby & Kagawa, 2020).

Second, the global economic losses resulting from the perfect storm increase with the scale of flooding, which is quite straightforward. However, some regions may see opposite changes in their GVA losses. Regions closely trading with the flooded region experience the stimulus effect from the post-flood reconstruction activities, which, to some extent, offsets the side effect of the pandemic control. A similar stimulus effect is also found in the research of Koks and Thissen (2016) where substitution of suppliers is allowed.

Third, other factors which are positively correlated with the perfect storm's economic footprint are the spread and strictness of the pandemic control. When pandemic control takes place after flooding this leads to more severe economic impacts than when control is implemented before the flooding, due to longer-lasting disruption of the post-flood recovery. We also compare the impacts of a 30%-24 week pandemic control with a 60%-8 week pandemic control applied intermittently in the recovery period of multiple scales of flooding and discover that a stricter but shorter pandemic control could reduce the economic losses of all regions. This is in line with the major insight provided in the research of Guan et al. (2020).

Finally, when increasing trade barriers intertwines with the collision of flooding and pandemic control, it creates a triangled perfect storm. Our results illustrate that export restrictions increase economic losses in all regions and that these losses increase exponentially with the degree of the

export restriction. Specialization which leads to the concentration of key sectors in particular regions and limits possibilities for substitution raises the vulnerability of the economic network to such compound risks. Export restrictions imposed on the specialized sectors, can trigger devastating impacts on the global economy at a time when it is already heavily burdened by addressing the compound hazards of extreme weather events and pandemic control.

The findings of our research together suggest an integrated approach in tackling the compound risks of climate change and pandemic. By utilizing our compound-hazard impact model, people can grasp a better view of the economic interlinkages between multiple hazards which ultimately develop into a perfect storm. Knowing the constraints from one hazard while responding to another assists the formation of a balanced strategy which can minimize the economic losses from the trade-offs between emergency response and pandemic control.

Regional or global cooperation can help address the spillover effects of such compound events. Our results have illustrated how a region can benefit from another region's active reconstruction and strict virus containment, but there are also occasions when a region is negatively impacted by events and measures taken in response in other regions.. Our impact model has demonstrated its flexibility addressing various scenarios and can help governments refine their emergency policies by considering the potential positive or negative externalities on wider economic systems. This is of importance in the context of deglobalization. Policies that lead to higher trade barriers and undermine the efforts of other countries battling extreme weather events and a pandemic. The use of trade restrictions has a particularly deleterious impact in a world with production specialization in key sectors raising the need for effective discipline at the global level of the use of such measures..

Beyond these policy implications, our model also provides consistent and comparable loss metrics with that of single-hazard analysis, as it is based on the popular ARIO model in this field. This will facilitate comparison with future studies of a similar methodological framework. Nevertheless, the model is limited by not allowing for technical progress and is relevant for a short-term time scale, where the production patterns of economic sectors do not shift significantly. This outlook explains why we only consider the substitution between intermediate inputs of the same kind from different regions, rather than the substitution between different types of inputs. In addition, this model only focuses on the economic mechanisms through which different types of hazards interweave with each other. Specifically, we investigate the negative effects of pandemic control and trade restrictions on post-flood economic recovery. Admittedly, there are other kinds of interaction between natural and biological hazards, it is not in our scope to model all these factors. For example, some response measures towards flooding, such as evacuation and displacement, could increase the number of people exposed to the pandemic and the burden on the healthcare system. The health-related interaction mechanism and the consequent economic costs could be incorporated into future studies.

## Appendix

**Table S1. A sample input-output table (IOT) of a hypothetical global economy with 4 regions and 5 sectors.** The values are given in million US dollars at 2015 prices. AGR, MANG, MANR, CON and OTH refer to the five sectors of agriculture, general manufacturing, capital manufacturing, construction, and other services, respectively.

| | | Intermediate Use | | | | | | | | | | | | | | | | | | | | Final Use | | | | Output |
|---|---|---|---|---|---|---|---|---|---|---|---|---|---|---|---|---|---|---|---|---|---|---|---|---|---|---|
| | | A | | | | | B | | | | | C | | | | | D | | | | | | | | | |
| | | AGR | MANG | MANR | CON | OTH | AGR | MANG | MANR | CON | OTH | AGR | MANG | MANR | CON | OTH | AGR | MANG | MANR | CON | OTH | A | B | C | D | |
| A | AGR | 801 | 2602 | 4 | 61 | 326 | 62 | 275 | 1 | 27 | 73 | 87 | 385 | 0 | 6 | 14 | 16 | 34 | 0 | 1 | 6 | 1145 | 290 | 108 | 31 | 6356 |
| | MANG | 1178 | 14069 | 2455 | 3057 | 3401 | 113 | 2848 | 729 | 655 | 361 | 67 | 1355 | 165 | 135 | 167 | 39 | 524 | 123 | 206 | 111 | 2394 | 456 | 211 | 183 | 35003 |
| | MANR | 73 | 1220 | 3643 | 632 | 1089 | 5 | 42 | 419 | 48 | 65 | 4 | 67 | 322 | 33 | 70 | 2 | 28 | 83 | 31 | 36 | 3267 | 263 | 760 | 203 | 12407 |
| | CON | 1 | 48 | 11 | 154 | 192 | 0 | 1 | 1 | 4 | 2 | 0 | 1 | 0 | 12 | 2 | 0 | 1 | 0 | 3 | 2 | 8518 | 134 | 234 | 192 | 9515 |
| | OTH | 350 | 5083 | 1594 | 1621 | 10395 | 40 | 905 | 528 | 436 | 1356 | 23 | 548 | 192 | 229 | 385 | 22 | 206 | 73 | 121 | 299 | 13772 | 1250 | 578 | 671 | 40677 |
| B | AGR | 16 | 81 | 0 | 2 | 13 | 613 | 3385 | 10 | 333 | 645 | 46 | 202 | 0 | 3 | 7 | 8 | 18 | 0 | 0 | 3 | 34 | 1974 | 56 | 16 | 7466 |
| | MANG | 116 | 964 | 182 | 338 | 664 | 1256 | 35356 | 8867 | 6541 | 5662 | 98 | 1237 | 216 | 246 | 362 | 61 | 714 | 155 | 272 | 326 | 937 | 9719 | 744 | 669 | 75701 |
| | MANR | 13 | 281 | 812 | 238 | 625 | 87 | 2179 | 17343 | 1880 | 2241 | 11 | 310 | 967 | 217 | 267 | 6 | 139 | 441 | 141 | 203 | 2039 | 11388 | 3043 | 1089 | 45959 |
| | CON | 0 | 6 | 2 | 35 | 38 | 13 | 115 | 42 | 1312 | 254 | 1 | 6 | 1 | 59 | 11 | 0 | 3 | 0 | 15 | 10 | 2585 | 14795 | 1150 | 945 | 21399 |
| | OTH | 8 | 324 | 133 | 122 | 740 | 390 | 9538 | 5629 | 3903 | 21503 | 21 | 608 | 216 | 206 | 562 | 18 | 253 | 86 | 149 | 436 | 794 | 24501 | 856 | 648 | 71646 |
| C | AGR | 21 | 105 | 0 | 2 | 17 | 42 | 189 | 1 | 19 | 50 | 1451 | 5403 | 7 | 116 | 275 | 11 | 24 | 0 | 1 | 4 | 46 | 207 | 2454 | 22 | 10466 |
| | MANG | 117 | 857 | 190 | 498 | 533 | 130 | 2954 | 1118 | 1268 | 490 | 1913 | 33380 | 5253 | 5454 | 3788 | 54 | 621 | 191 | 430 | 209 | 413 | 623 | 6271 | 284 | 67040 |
| | MANR | 7 | 102 | 190 | 70 | 128 | 11 | 91 | 522 | 89 | 90 | 44 | 2098 | 7998 | 878 | 1108 | 5 | 54 | 119 | 51 | 50 | 478 | 304 | 8631 | 265 | 23384 |
| | CON | 0 | 2 | 1 | 9 | 10 | 0 | 2 | 1 | 6 | 3 | 7 | 156 | 41 | 538 | 197 | 0 | 1 | 0 | 4 | 3 | 700 | 174 | 12524 | 256 | 14634 |
| | OTH | 4 | 102 | 51 | 36 | 225 | 22 | 409 | 230 | 169 | 649 | 334 | 6942 | 2263 | 2614 | 8653 | 9 | 102 | 39 | 65 | 177 | 434 | 691 | 14909 | 395 | 39524 |
| D | AGR | 17 | 87 | 0 | 2 | 14 | 34 | 154 | 1 | 15 | 41 | 48 | 214 | 0 | 3 | 8 | 699 | 1438 | 1 | 22 | 189 | 37 | 167 | 62 | 1185 | 4439 |
| | MANG | 40 | 412 | 65 | 116 | 139 | 41 | 1466 | 390 | 293 | 172 | 30 | 736 | 82 | 103 | 97 | 611 | 7500 | 1174 | 2401 | 1561 | 116 | 198 | 94 | 2293 | 20131 |
| | MANR | 1 | 31 | 92 | 21 | 64 | 2 | 17 | 253 | 16 | 33 | 2 | 35 | 188 | 21 | 49 | 13 | 408 | 2493 | 418 | 456 | 224 | 174 | 533 | 2015 | 7562 |
| | CON | 0 | 1 | 0 | 7 | 7 | 0 | 1 | 1 | 4 | 2 | 0 | 1 | 0 | 11 | 2 | 1 | 26 | 8 | 160 | 87 | 502 | 128 | 223 | 6581 | 7755 |
| | OTH | 2 | 63 | 29 | 22 | 158 | 11 | 237 | 131 | 95 | 420 | 6 | 142 | 52 | 50 | 110 | 224 | 2503 | 947 | 1077 | 3924 | 224 | 391 | 187 | 6809 | 17811 |
| Value-added | Capital | 248 | 2907 | 819 | 294 | 4813 | 130 | 4847 | 2221 | 315 | 9160 | 198 | 4389 | 1254 | 397 | 5743 | 144 | 2003 | 382 | 139 | 2085 | | | | | |
| | Labour | 3342 | 5657 | 2133 | 2179 | 17083 | 4464 | 10688 | 7522 | 3971 | 28376 | 6077 | 8823 | 4166 | 3304 | 17648 | 2494 | 3531 | 1245 | 2049 | 7634 | | | | | |
| Input | | 6356 | 35003 | 12407 | 9515 | 40677 | 7466 | 75701 | 45959 | 21399 | 71646 | 10466 | 67040 | 23384 | 14634 | 39524 | 4439 | 20131 | 7562 | 7755 | 17811 | | | | | |

**Table S2. Capital matrix.** Products required to rebuild one unit of capital in each region.

| Region-Sector | | A | B | C | D |
|---|---|---|---|---|---|
| A | AGR | 0 | 0 | 0 | 0 |
| | MANG | 0 | 0 | 0 | 0 |
| | MANR | 0.15 | 0 | 0.02 | 0 |
| | CON | 0.61 | 0 | 0 | 0 |
| | OTH | 0 | 0 | 0 | 0 |
| B | AGR | 0 | 0 | 0 | 0 |
| | MANG | 0 | 0 | 0 | 0 |
| | MANR | 0.06 | 0.25 | 0.06 | 0 |
| | CON | 0.12 | 0.7 | 0.04 | 0 |
| | OTH | 0 | 0 | 0 | 0 |
| C | AGR | 0 | 0 | 0 | 0 |
| | MANG | 0 | 0 | 0 | 0 |
| | MANR | 0.02 | 0.05 | 0.2 | 0 |
| | CON | 0.04 | 0 | 0.68 | 0 |
| | OTH | 0 | 0 | 0 | 0 |
| D | AGR | 0 | 0 | 0 | 0 |
| | MANG | 0 | 0 | 0 | 0 |
| | MANR | 0 | 0 | 0 | 0.3 |
| | CON | 0 | 0 | 0 | 0.7 |
| | OTH | 0 | 0 | 0 | 0 |

## References


AghaKouchak, A., Chiang, F., Huning, L. S., Love, C. A., Mallakpour, I., Mazdiyasni, O., . . . Sadegh, M. (2020). Climate Extremes and Compound Hazards in a Warming World. *Annual Review of Earth and Planetary Sciences, 48*(1), 519-548. doi:10.1146/annurev-earth-071719-055228

Bénassy, J.-P. (1993). Nonclearing Markets: Microeconomic Concepts and Macroeconomic Applications. *Journal of Economic Literature, 31*(2), 732-761.

Christoph E. Boehm , Aaron Flaaen , and Nitya Pandalai-Nayar (2019) Input Linkages and the Transmission of Shocks: Firm-Level Evidence from the 2011 Tōhoku Earthquake, The Review of Economics and Statistics 2019 101:1, 60-75 https://www.mitpressjournals.org/doi/abs/10.1162/rest_a_00750

Boyle, L. (2020). 2020 has been a bleak year in the climate crisis. So here's the good news. Retrieved from https://www.independent.co.uk/environment/climate-change/climate-change-2020-record-good-news-b1780393.html

Bubeck, P., Otto, A., & Weichselgartner, J. (2017). Societal Impacts of Flood Hazards. In: Oxford University Press.

Chondol, T., Bhardwaj, S., Panda, A. K., & Gupta, A. K. (2020). Multi-Hazard Risk Management During Pandemic. In *Integrated Risk of Pandemic: Covid-19 Impacts, Resilience and Recommendations* (pp. 445-461). Singapore: Springer Singapore.

ESCAP. (2019). *Asia-Pacific Disaster Report 2019*. Retrieved from Economic and Social Commission for Asia and the Pacific, United Nations: https://www.unescap.org/publications/asia-pacific-disaster-report-2019

Espitia, A., Rocha, N., & Ruta, M. (2020). *Covid-19 and Food Protectionism: The Impact of the Pandemic and Export Restrictions on World Food Markets*: The World Bank.

Field, C. B., Barros, V., Stocker, T. F., & Dahe, Q. (2012). *Managing the risks of extreme events and disasters to advance climate change adaptation: special report of the Intergovernmental Panel on Climate Change*. Cambridge, UK: Cambridge University Press.

Gohd, C. (2021). 2020 ties record for the hottest year ever, NASA analysis shows. Retrieved from https://www.space.com/nasa-confirms-2020-hottest-year-on-record

Guan, D., Wang, D., Hallegatte, S., Davis, S. J., Huo, J., Li, S., . . . Gong, P. (2020). Global supply-chain effects of COVID-19 control measures. *Nature Human Behaviour, 4*(6), 577-587. doi:10.1038/s41562-020-0896-8

Hallegatte, S. (2008). An adaptive regional input-output model and its application to the assessment of the economic cost of Katrina. *Risk Analysis, 28*(3), 779-799. Retrieved from <Go to ISI>://WOS:000256858800018

Hallegatte, S. (2014). Modeling the Role of Inventories and Heterogeneity in the Assessment of the Economic Costs of Natural Disasters. *Risk Analysis, 34*(1), 152-167. doi:https://doi.org/10.1111/risa.12090

Hao, Z., AghaKouchak, A., & Phillips, T. J. (2013). Changes in concurrent monthly precipitation and temperature extremes. *Environmental Research Letters, 8*(3), 034014. doi:10.1088/1748-9326/8/3/034014

Hariri-Ardebili, M. A. (2020). Living in a Multi-Risk Chaotic Condition: Pandemic, Natural Hazards and Complex Emergencies. *International Journal of Environmental Research and Public Health, 17*(16). doi:10.3390/ijerph17165635

Ishiwatari, M., Koike, T., Hiroki, K., Toda, T., & Katsube, T. (2020). Managing disasters amid COVID-19 pandemic: Approaches of response to flood disasters. *Progress in Disaster Science, 6*, 100096. doi:https://doi.org/10.1016/j.pdisas.2020.100096

Johnstone, W. M., & Lence, B. J. (2009). Assessing the value of mitigation strategies in reducing the impacts of rapid-onset, catastrophic floods. *Journal of Flood Risk Management, 2*(3), 209-221. doi:https://doi.org/10.1111/j.1753-318X.2009.01035.x

Koks, E. E., Bockarjova, M., De Moel, H., & Aerts, J. C. J. H. (2015). Integrated direct and indirect flood risk modeling: development and sensitivity analysis. *Risk Analysis, 35*(5), 882-900. Retrieved from <Go to ISI>://WOS:000356706800010

Koks, E. E., & Thissen, M. (2016). A multiregional impact assessment model for disaster analysis. *Economic Systems Research, 28*(4), 429-449. Retrieved from https://doi.org/10.1080/09535314.2016.1232701

Laframboise, N., & Loko, B. (2012). *Natural Disasters: Mitigating Impact, Managing Risks*. IMF Working Paper No. 12/245. Retrieved from https://papers.ssrn.com/sol3/papers.cfm?abstract_id=2169784

Lenzen, M., Malik, A., Kenway, S., Daniels, P., Lam, K. L., & Geschke, A. (2019). Economic damage and spillovers from a tropical cyclone. *Natural Hazards and Earth System Sciences, 19*(1), 137-151. doi:10.5194/nhess-19-137-2019

Leonard, M., Westra, S., Phatak, A., Lambert, M., van den Hurk, B., McInnes, K., . . . Stafford-Smith, M. (2014). A compound event framework for understanding extreme impacts. *Wiley Interdisciplinary Reviews: Climate Change, 5*(1), 113-128. doi:https://doi.org/10.1002/wcc.252

McKibbin, W. J., & Fernando, R. (2020). *The Global Macroeconomic Impacts of COVID-19: Seven Scenarios*. CAMA Working Paper No. 19/2020. Retrieved from https://papers.ssrn.com/sol3/papers.cfm?abstract_id=3547729

Miller, R. E., & Blair, P. D. (2009). *Input-output analysis: foundations and extensions*: Cambridge university press.

Okuyama, Y., & Santos, J. R. (2014). Disaster impact and input-output analysis. *Economic Systems Research, 26*(1), 1-12. Retrieved from https://doi.org/10.1080/09535314.2013.871505

Oosterhaven, J., & Bouwmeester, M. C. (2016). A new approach to modeling the impact of disruptive events. *Journal of Regional Science, 56*(4), 583-595. Retrieved from https://doi.org/10.1111/jors.12262

Oosterhaven, J., & Többen, J. (2017). Wider economic impacts of heavy flooding in Germany: a non-linear programming approach. *Spatial Economic Analysis, 12*(4), 404-428. Retrieved from https://doi.org/10.1080/17421772.2017.1300680

Oxford Analytica. (2020). Pandemic-induced trade protectionism will persist. *Expert Briefings*. doi:https://doi.org/10.1108/OXAN-ES257613

Pei, S., Dahl, K. A., Yamana, T. K., Licker, R., & Shaman, J. (2020). Compound Risks of Hurricane Evacuation Amid the COVID-19 Pandemic in the United States. *GeoHealth, 4*(12), e2020GH000319. doi:https://doi.org/10.1029/2020GH000319

Phillips, C. A., Caldas, A., Cleetus, R., Dahl, K. A., Declet-Barreto, J., Licker, R., . . . Carlson, C. J. (2020). Compound climate risks in the COVID-19 pandemic. *Nature Climate Change, 10*(7), 586-588.

Rose, A. Z. (1995). Input-output economics and computable general equilibrium models. *Structural Change and Economic Dynamics, 6*(3), 295-304. Retrieved from http://www.sciencedirect.com/science/article/pii/0954349X95000018I

Rose, A. Z. (2004). Economic principles, issues, and research priorities in hazard loss estimation. In Y. Okuyama & S. E. Chang (Eds.), *Modelling Spatial and Economic Impacts of Disasters*. Berlin, Heidelberg: Springer.

Salas, R. N., Shultz, J. M., & Solomon, C. G. (2020). The Climate Crisis and Covid-19 - A Major Threat to the Pandemic Response. *New England Journal of Medicine, 383*(11), 70. doi:10.1056/NEJMp2022011

Sarkar-Swaisgood, M., & Srivastava, S. (2020). *When COVID-19 and Natural Hazards Collide: Building Resilient Infrastructure in South Asia*. Observer Research Foundation (ORF). Retrieved from

http://repo.floodalliance.net/jspui/handle/44111/3826

Selby, D., & Kagawa, F. (2020). Climate change and coronavirus: a confluence of crises as learning moment. In Pádraig Carmody, Gerard McCann, C. Colleran, & C. O'Halloran (Eds.), *COVID-19 in the Global South: Impacts and Responses*. UK: Bristol University Press.

Shahid, S. (2020). Deglobalization and its Discontents: The Pandemic Effect. Retrieved from https://economics.td.com/deglobalization-discontents

Shen, X., Cai, C., Yang, Q., Anagnostou, E. N., & Li, H. (2021). The US COVID-19 pandemic in the flood season. *Science of the Total Environment, 755*, 142634. doi:https://doi.org/10.1016/j.scitotenv.2020.142634

Shrabani, S. T., Udit, B., Mohit, P. M., Subhankar, K., & Subimal, G. (2021). Flood evacuation during pandemic: a multi-objective framework to handle compound hazard. *Environmental Research Letters*. Retrieved from http://iopscience.iop.org/article/10.1088/1748-9326/abda70

The Lancet. (2020). Editorial: a tale of two emergencies. *The Lancet. Planetary Health, 4*(3), 86.

UNFCCC. (2015). *Adoption of the Paris Agreement* (Report No. FCCC/CP/2015/L.9/Rev.1). Retrieved from United Nations Framework Convention on Climate Change, Paris, France: http://unfccc.int/resource/docs/2015/cop21/eng/l09r01.pdf

UNISDR. (2015). *Sendai framework for disaster risk reduction 2015-2030*. Retrieved from United Nations International Strategy for Disaster Reduction, Sendai, Japan: http://www.wcdrr.org/uploads/Sendai_Framework_for_Disaster_Risk_Reduction_2015-2030.pdf

Wenz, L., & Levermann, A. (2016). Enhanced economic connectivity to foster heat stress-related losses. *Science advances, 2*(6), e1501026-e1501026. doi:10.1126/sciadv.1501026

White, D. A. L. (2020). 2020 Atlantic Hurricane Season Most Active On Record: NOAA. Retrieved from https://www.msn.com/en-us/weather/topstories/2020-atlantic-hurricane-season-most-active-on-record-noaa/ar-BB1aStCW

Willner, S. N., Otto, C., & Levermann, A. (2018). Global economic response to river floods. *Nature Climate Change, 8*(7), 594-598. Retrieved from <Go to ISI>://WOS:000440200100018

World Health Organization (WHO). (2015). Climate change and human health. Retrieved from https://www.who.int/globalchange/global-campaign/cop21/en/

Xia, Y., Li, Y., Guan, D., Tinoco, D. M., Xia, J., Yan, Z., . . . Huo, H. (2018). Assessment of the economic impacts of heat waves: A case study of Nanjing, China. *Journal of Cleaner Production, 171*,

811-819. doi:https://doi.org/10.1016/j.jclepro.2017.10.069

Zeng, Z., & Guan, D. (2020). Methodology and application of flood footprint accounting in a hypothetical multiple two-flood event. *Philosophical Transactions of the Royal Society A: Mathematical, Physical and Engineering Sciences, 378*(2168), 20190209. doi:http://10.1098/rsta.2019.0209

Zeng, Z., Guan, D., Steenge, A. E., Xia, Y., & Mendoza-Tinoco, D. (2019). Flood footprint assessment: a new approach for flood-induced indirect economic impact measurement and post-flood recovery. *Journal of Hydrology, 579*, 124204. doi:https://doi.org/10.1016/j.jhydrol.2019.124204

Zheng, H., Zhang, Z., Wei, W., Song, M., Dietzenbacher, E., Wang, X., . . . Guan, D. (2020). Regional determinants of China's consumption-based emissions in the economic transition. *Environmental Research Letters, 15*(7), 074001.

Zscheischler, J., Westra, S., van den Hurk, B. J. J. M., Seneviratne, S. I., Ward, P. J., Pitman, A., . . . Zhang, X. (2018). Future climate risk from compound events. *Nature Climate Change, 8*(6), 469-477. doi:10.1038/s41558-018-0156-3